Physical and Electrical Characterization of Aluminum Polymer Capacitors

David Liu
MEI Technologies, Inc.
NASA Goddard Space Flight Center
Greenbelt, MD 20771
Phone: 301-286-8573
Donhang.liu-1@nasa.gov

Michael J. Sampson
NASA Goddard Space Flight Center
Greenbelt, MD 20771
Phone: 301-286-3335
Michael.J.Sampson@nasa.gov

ABSTRACT

Polymer aluminum capacitors from several manufacturers with various combinations of capacitance, rated voltage, and ESR values were physically examined and electrically characterized. The physical construction analysis of the capacitors revealed three different capacitor structures, i.e., traditional wound, stacked, and laminated.

Electrical characterization results of polymer aluminum capacitors are reported for frequency-domain dielectric response at various temperatures, surge breakdown voltage, and other dielectric properties. The structure-property relations in polymer aluminum capacitors are discussed.

INTRODUCTION

The increasing speed and power usage in today's electronic circuitry lead to a strong demand on capacitors with high capacitance and low ESR and low ESL at high frequencies. The solid tantalum and aluminum electrolyte capacitors, with highly conductive polymers such as tetracyano-quinodimethane (TCNQ), polypyrole (PPY), and polyethylene-dioxythiophene (PEDT) as cathode materials exhibiting extremely low ESR and high capacitance at high frequencies, meet the requirements.

Thorough studies on the characterization of tantalum polymer capacitors for high reliability aerospace application have been reported previously [1-2]. Although the initial driving force for the development of polymer capacitors is to reduce the ESR, the results are more compelling than ESR itself. The polymer capacitors also exhibit improved performance such as faster dynamic transient response, better ripple voltage smoothing, superior reliability, and open-circuit, ignition-free failure mechanism. As a result, the polymer capacitors have been considered a competitive substitute of MnO_2-based solid tantalum and wet aluminum electrolyte capacitors, particularly at low voltage (<16V) applications.

In this paper, the focus will be primarily on the structure-property relations in polymer aluminum (PA) capacitors with emphasis on dielectric properties. The long-term reliability evaluation and qualification of these PA capacitors for potential aerospace applications will be report elsewhere.

PHYSICAL STRUCTURES OF POLYMER ALUMINUM CAPACITORS

In the fabrication of tantalum polymer capacitors, the polymer is a straight substitution of the MnO_2 in the capacitor assembly. The material change in tantalum polymer capacitor processing did not change the structure of the capacitor device.

On the other hand, a variety of processing changes has been made in manufacturing PA capacitors [3-6]. An early version of PA capacitor processing adapted the traditional wound technique with a polymer material replacing the wet electrolyte. However, it is not a simple replacement of polymer to the wet electrolyte due to the brittleness of the solidified polymer coating. Unlike the wound structure for wet electrolyte in which all foil layers can be wound together tightly, the polymer rolled foils were wound loosely in order to reserve a large gap to prevent the rubbing between cathode foil and anode film to cause a short circuit [5].

As an alternative, a "stacked" construction of PA capacitors was developed in recent years in which the etched and anodized aluminum foils are stacked and bonded together into a single structure. The anode lead frame is welded to the bond area of aluminum plate, while the cathode construction with coating of carbon and silver epoxy for terminal connection is similar to that solid tantalum capacitor utilizes [5,6]. This design facilitates the surface mount termination and utilizes the capacitor spacing more effectively, and therefore is adapted by many manufacturers.

In order to investigate the impacts of capacitor construction techniques on the electrical performance, a number of commercially available PA capacitors were selected and purchased from 5 different manufacturers. A product or a manufacturer was selected based upon the following criteria: (1). a manufacturer shall be a primary supplier in polymer capacitor products. (2). the capacitor has a unique design with competitive performance. (3). all capacitors purchased have the same footprint to facilitate the use of single PCB testing circuit.

Figure 1 combines the cross-section optical view and the top and side radiographic views of a 180 μF, 6.3V PA capacitor made by manufacturer A. This is a commercial grade PA capacitor with a total of 15 layers of etched and anodized aluminum foil "stacked". The capacitor body was encapsulated by an epoxy molding with a typical thickness of 10 μm for the side margin and 15 μm for the cover plate. The PA capacitors from manufacturer D was also found with the same "stacked" construction.

The energy dispersive X-ray (EDX) dot mapping images and the cross-section electron scanning microscope (SEM) have been used to examine the physical structures of PA capacitors. Figure 2 shows EDX and SEM images of the end of single foils from the stack at high magnifications. This commercial part uses a 13-μm thick anodized aluminum foil with an etched tunnel having a typical depth of ~4.5 μm at both sides of the foil. The cathode construction consisting of an over coating of carbon (graphite) followed by a silver layer bonding to the outside lead frame. The EDX mapping also reveals that the dominant elements in the conducting polymer coating are sulfur and carbon.

Figure 3 and 4 summarize the construction analysis results for a 100 μF, 6.0 V PA capacitor made by manufacturer E. The capacitor adapts a unique "laminated" structure that is totally different from previously described PA capacitor structural details. The anodized aluminum foil has a substantial big thickness of 30 μms, while the etched tunnel depth is about 13 μm on each side of the aluminum foil. The aluminum foil was only etched selectively. The non-etched end of the aluminum foil was wire-bonded directly to the lead frame for the formation of anode. The cathode, on the other hand, was formed using a nickel coated copper plate which is then sandwiched between two anodized aluminum foils.

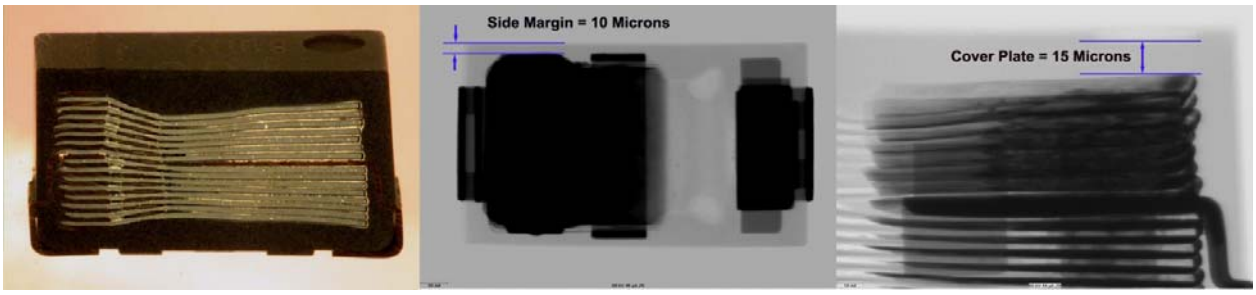

Figure 1. Optical cross-section view (left) and the top (middle) and side (right) radiographic views of a 180 μF, 6.3V polymer aluminum capacitor made by manufacturer A show a "stacked" structure.

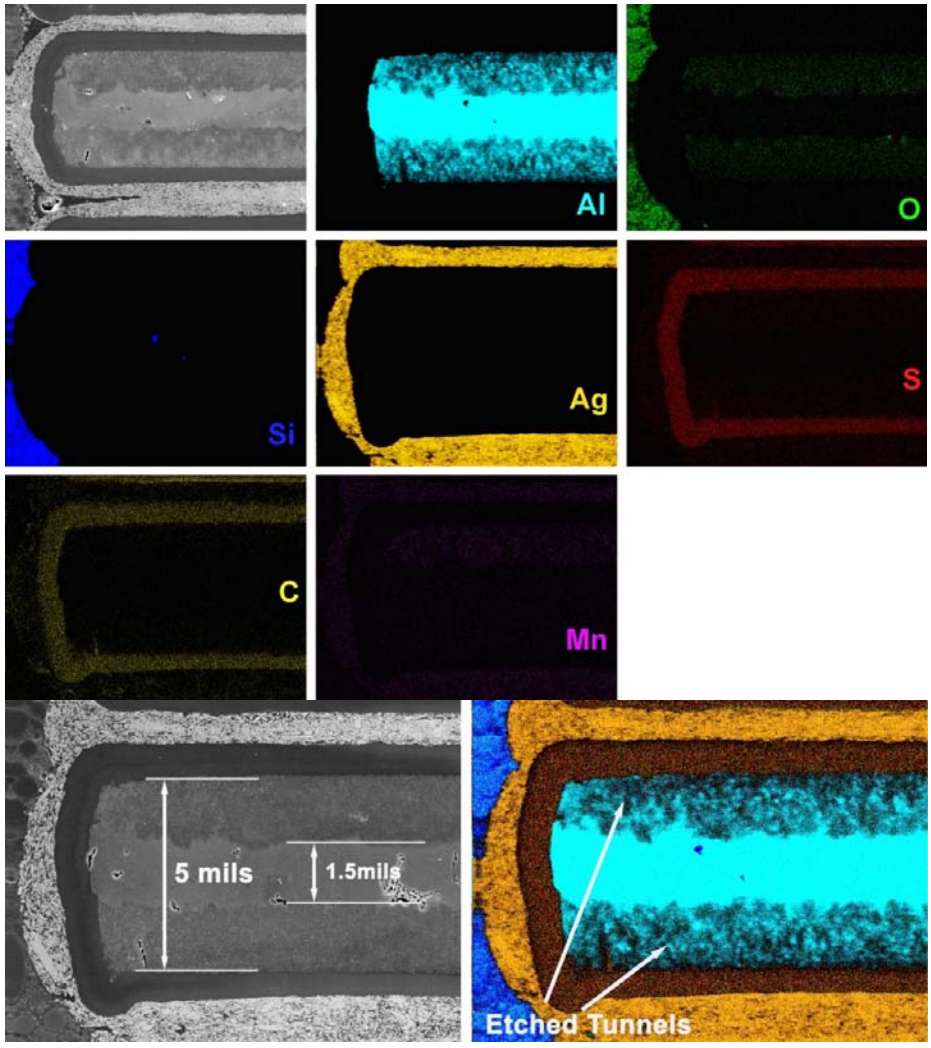

Figure 2. Two-dimensional EDX mapping results and cross-section SEM images show the end of single foils from the stack at high magnification for a 180 μF, 6.3V PA capacitor made by manufacturer A.

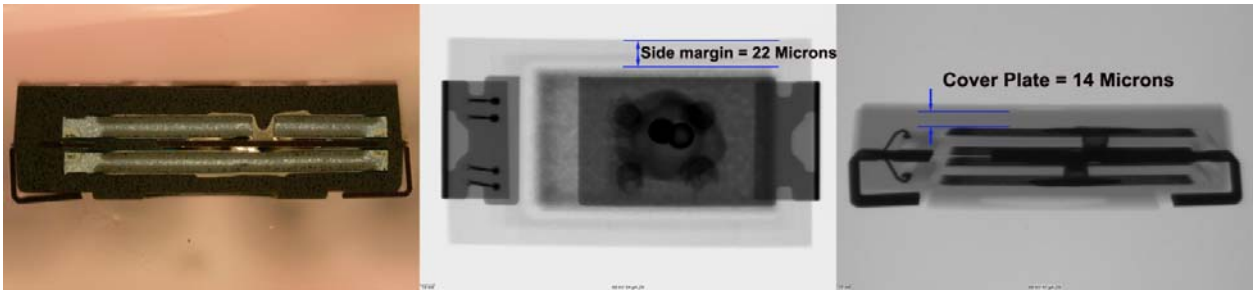

Figure 3. Optical cross-section view (left) and the top (middle) and side (right) radiographic views of a 100 μF, 6V polymer aluminum capacitor made by manufacturer E show a "laminated" structure.

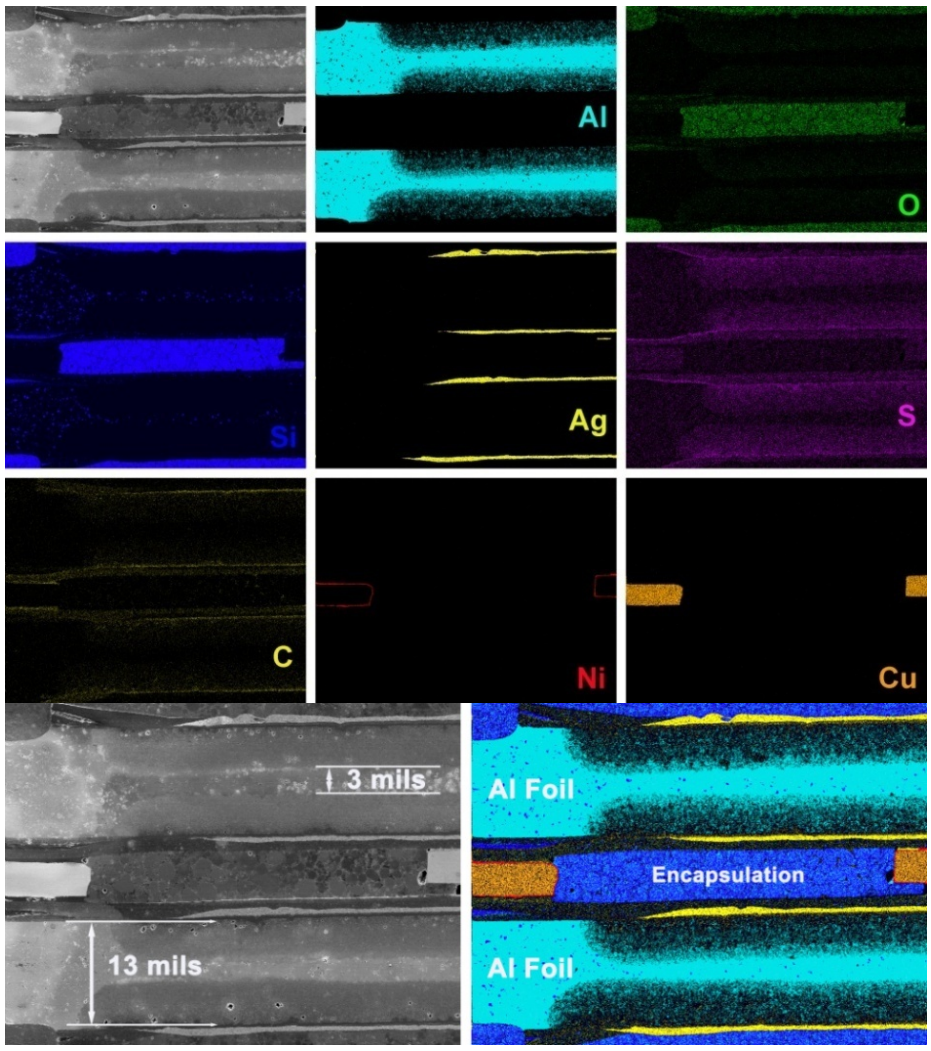

Figure 4. Two-dimensional EDX mapping results and cross-section SEM images of a 100 μF, 6V PA capacitor made by manufacturer E show a "laminated" structure.

Figure 5. External and cross-section optical views of a 100 μF, 10V PA capacitor made by manufacturer C.

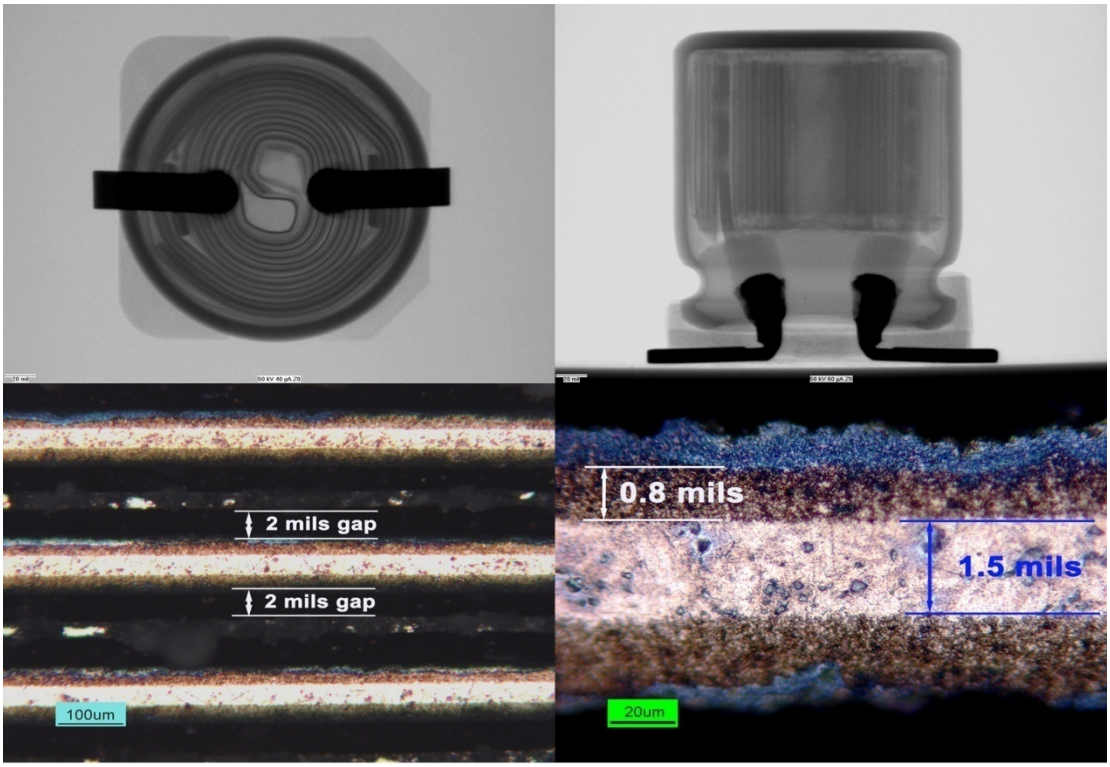

Figure 6. Radiographic images and high-magnification cross-sectional optical views of a 100 μF, 10 V PA capacitor made by manufacturer C show a traditional "wound" structure.

This unique "laminated" structure leads to a very low ESR value (5 mΩ specified). Since only two layers of aluminum foil were used, this capacitor also has the smallest profile among all the capacitors reported in this paper.

The construction analysis of a 100 μF, 10V capacitor made by manufacturer C is summarized in Figures 5 and 6 respectively. The results reveal that the capacitor was constructed using a traditional "wound" structure that is conventionally used for wet electrolyte aluminum capacitors. A square plastic base was assembled at the bottom of the capacitor body, so that both anode and cathode leads can be tilted 90 degrees to achieve a surface mounting capability.

As mentioned before, in order to prevent potential rubbing of cathode foil against the anode film and creating a "short-circuit" failure, a spacer is required during the foil winding. Indeed, as shown in Figure 5, the foils were wound together so loosely that a ~5 μm (2 mils) gap was created between each cathode and anode films. The existence of the gap makes the SEM and EDX examination almost impossible for this capacitor, since the foils keep drifting around when a high energy electron beam was applied to the foil material. The high-magnification optical examination reveals that anodized foil in this 10 V rated capacitor has a typical thickness of ~8.2 μm with etched tunnel depth of ~2.0 μm at both sides of the foil.

ELECTRICAL CHARACTERIZATION

1. Dielectric properties

All capacitors were solder-reflow attached on the testing board prior to testing. Each testing board holds 20 pieces of surface mount PA capacitors. The soldering reflow condition follows MIL-PRF-55365G. No-clean solder paste with RMA flux was used. Only one reflow cycle was applied.

It has been noticed that successive heat and long exposure to high temperature generated in an inappropriate solder reflow step may damage the polymer, cause early failures in MnO_2 tantalum capacitor, and deteriorate the capacitor's long term reliability. A proper reflow procedure will assure the good electrical contact and consistency in electrical characterizations.

The capacitors after reflow were tested completely for capacitance, dielectric loss, ESR, and DC leakage, in order to eliminate any possible early failures related to solder reflow process. The electrical testing follows the specification in MIL-PRF-55365G for tantalum capacitors, i.e., capacitance and DF at 120Hz and 1 V_{rms}, ESR at 100 kHz, and DC leakage current at rated voltage with 5 minutes discharge time. A 12 hours burn-in at 85°C was performed prior to electrical testing.

All measured electrical parametric data are shown in Figures 7. The data are presented in the format of a Weibull statistical plot with the y-axis scaled for normal probability and the x-axis for specific parameters.

All capacitors were found to show a tight distribution in capacitance (upper left plot in Figure 7). This is due to all capacitors were 100% tested at manufacturers prior to delivery. The value of slope β in Weibull plot here is relevant to the distribution of the parameter being tested. The higher the value of β, the tighter the measured parameter distribution.

Dielectric loss (DF) data of capacitors are also summarized in Figure 7 (upper right plot). All measured capacitors exhibit comparable dielectric loss. The PA capacitors with a "wound" structure from manufacturer C showed highest dielectric loss in the group.

The 100 kHz ESR data of these capacitors are shown in the lower left plot in Figure 7. All polymer capacitors showed comparable ESR results. In addition, most of the capacitors had ESR readings as specified in manufacturer's datasheet. ESR values as low as 3 mΩ were recorded for a 6.3V, 180 μF capacitor made by manufacturer A with a "stacked "structure. In addition, ESR values with various structures are statistically uniform with close β values, which may suggests that ESR value of a PA capacitor has little to do with the capacitor structure but solely depends on the characteristics of the cathode conducting polymer coating layer.

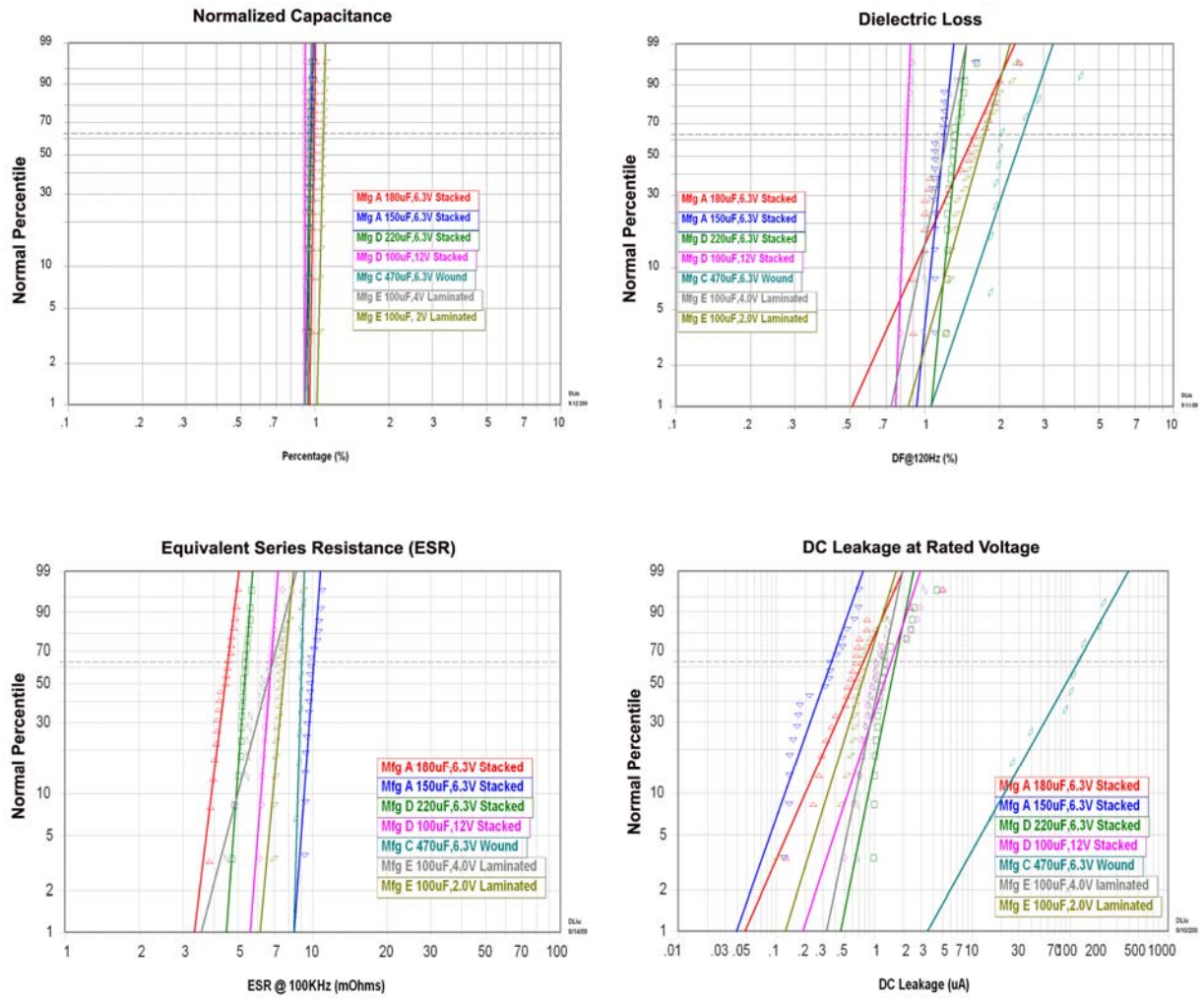

Figure 7. Weibull statistic plots of normalized dielectric properties for all the capacitor samples in this study.

The DC leakage current was tested for all PA capacitors at their rated voltages with 5 minutes charge time as specified in MIL-PRF-55365G. Most of PA capacitors tested exhibit DC leakage in the range of 0.1-1 μA with one exception: a 6.3V, 470 μF PA capacitor made by manufacturer C with a "wound" structure showed highest DC leakage current over 200 μA. Whether the wound construction, or the highest capacitance value among the group are the possible cause for the high leakage observed, is not confirmed.

2. Frequency-Domain Dielectric Response versus Capacitor Structures

In this paper, the PA capacitors are characterized using an Agilent 4294A Precision Impedance Analyzer in the frequency range from 100Hz to 10MHz. The RF testing fixtures are 4-terminal, 1-meter cable assemblies of which the high-frequency performance is optimized. The capacitor samples are electrically selected prior to being soldered at the ends of the RF cable assembly. The temperature range of frequency-domain characterization for PA

capacitors could be extended on the cold side beyond the normal military range of -55°C to 125°C because, unlike traditional aqueous based systems, polymer electrolytes cannot freeze.

The frequency-domain dielectric characterization of all PA capacitors tested showed that the capacitors with same physical structure exhibited very similar dielectric response. So that for the purpose of comparison simplicity, only one PA capacitor's RF testing data is presented for each PA capacitor structure.

Figure 8 shows capacitance and ESR versus frequency for a PA capacitor with 150 μF, 6.3 V rated voltage and a "stacked" structure made by manufacturer A. The ESR value at 100 kHz is about 8 mΩ (specified ESR is 12 mΩ).

As shown in Figure 8, the PA capacitor exhibits a constant response with frequency and slight dependence on temperature change. No capacitance roll-off is observed up to 200 kHz. ESR versus frequency curves show a "bath tub" shape with ESR falling at lower frequencies, leveling off at the middle frequencies, and rising slightly at higher frequencies. This ESR versus frequency change can be explained briefly as following: Total ESR comprises contributions from both dielectric loss of the oxide film which falls rapidly with increasing frequency and contact resistance in the electrolyte layers of conducting polymer which are typically constant with frequency. As frequency goes around 1MHz, skin effect becomes dominant which result in resistance increase with frequency.

Figure 9 shows capacitance and ESR versus frequency for a 470 μF, 6.3V and with loose "wound" structure made by manufacturer C. The roll-off of capacitance is evident for this device beginning at about 100 kHz. The lower frequency of capacitance roll-off (100 kHz) may have been contributed by the loose wound structure of the capacitor with extraordinary high dielectric loss and DC leakage as shown in Figure 7.

The capacitance and ESR versus frequency is shown in Figure 10 for a 100 μF, 4V capacitor with a "laminated" structure made by manufacturer E. The capacitance values at various temperatures exhibit nearly perfect straight lines versus frequency and do not change much with temperature. The capacitance at 100 kHz only decreased from 93.4 μF at +125°C to 80.8 μF at -95°C, a 13.5% decrease with a broad temperature range of more than 200°C. The measured value of ESR of 6.4 mΩ is slightly higher than the specified value of 5 mΩ, but this is not considered a significant difference. No capacitance roll-off was observed even up to 300 kHz. In addition, the ESR of the device shows stable low values over a board range of frequencies (1 – 1000 kHz).

The PA capacitor with "laminated" structure appears to be the best in dielectric performance versus both temperature and frequency among all three PA capacitor structures revealed.

3. Surge Breakdown Voltage Testing

As reported before, a prevalent failure for MnO_2- based tantalum capacitors is the power-on failures. The capacitor can be electrically broken down even below the rated voltage due to rapidly changed, high current turn-on pulses (a surge current). A test that is designed and applied to screen out these early failures has been widely applied to tantalum capacitors. This test is called steady step surge test (SSST test) [7].

This test consists of rapidly charging the capacitors with incremented voltage through low series resistance. All capacitors under test were solder-reflow assembled to a PCB test card prior to SSST test. When test begins, the capacitor is charged to a set voltage, held at that voltage for ½ second, and then discharged through a low resistor (~ 0.5 Ω) for ½ second. This sequence is repeated five times.

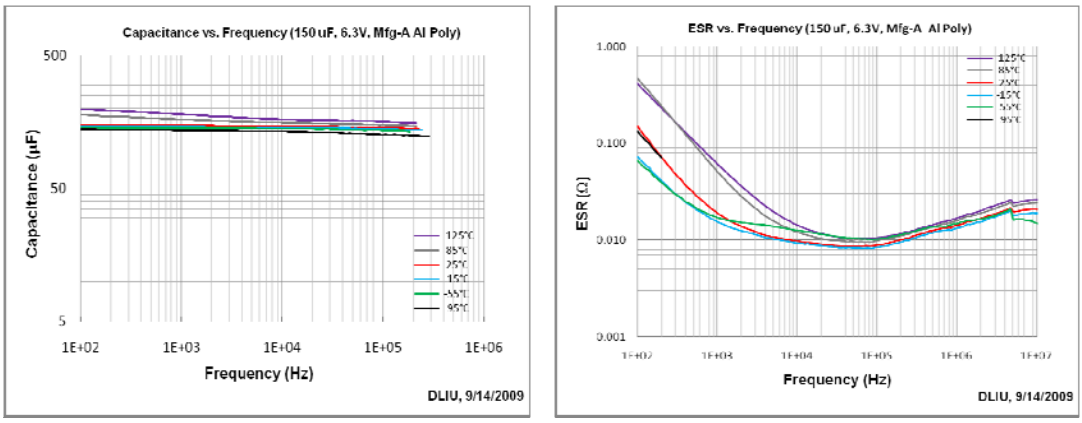

Figure 8. Capacitance and ESR vs. Frequency at Various Temperatures for a 6.3V, 180 µF Aluminum Polymer Capacitors with a "stacked" structure from manufacturer A.

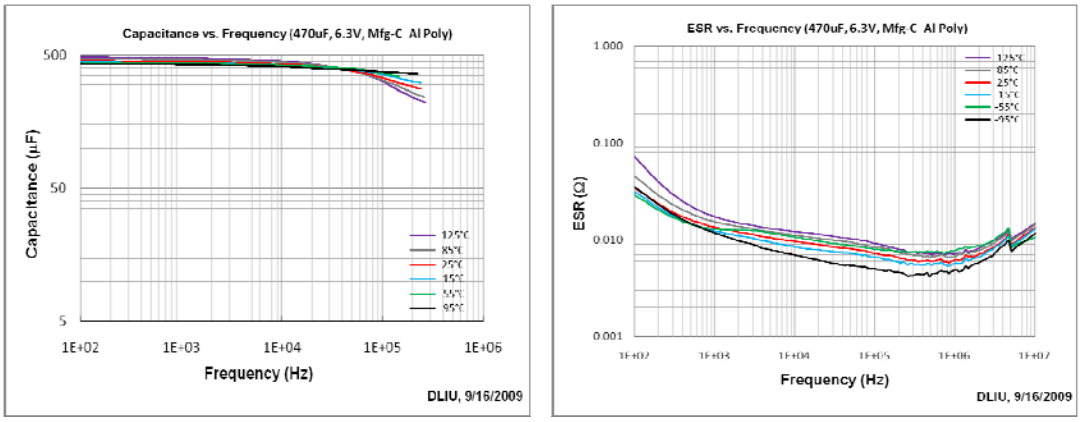

Figure 9. Capacitance and ESR vs. frequency at various temperatures for 6.3V, 470 µF PA capacitor with a loose "wound" structure from manufacturer C.

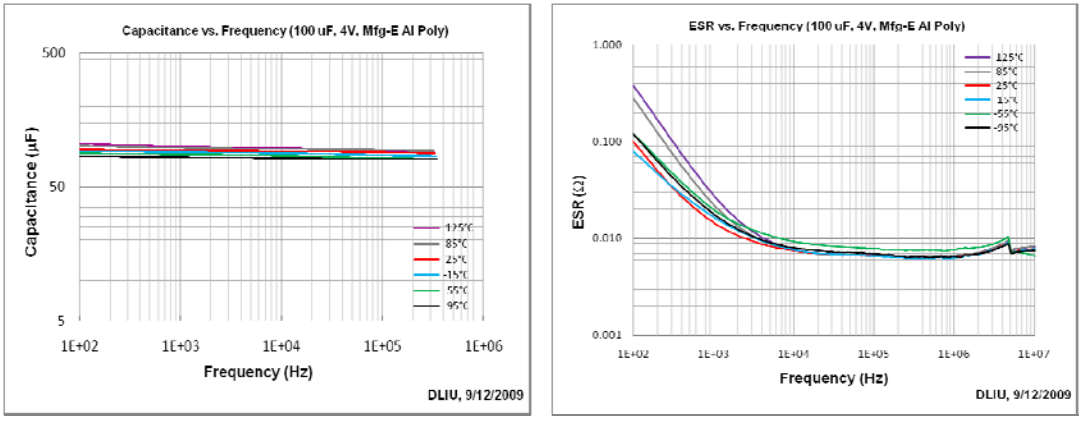

Figure 10. Capacitance and ESR vs. Frequency at Various Temperatures for 4V 100 µF PA Capacitor with a "laminated" structure from Manufacturer E. Note the measured capacitance is almost completely independent of temperature and frequency.

The voltage at which each capacitor in a sample fails is recorded and the percentage of failures is plotted versus breakdown voltage on a Weibull probability scale. For ease of comparison, the breakdown voltages are normalized with respect to the rated voltage.

Figure 11 compares a number of PA capacitors with rated voltage of 6.3V and below made by different manufacturers with all three capacitor structures included. The worst SSST breakdown voltage is found to be the 470 μF capacitor with a "wound" structure made by manufacturer C. The breakdown voltages in this capacitor range from 11.0V to 12.5V or 1.75 to 2.0 times of rated voltage, a range of 1.14:1. Such low values in breakdown voltage suggest that the "wound" structure is not a compelling technology for the construction of PA capacitors.

Other PA capacitors with "stacked" and "laminated" structures show breakdown voltages range from 2.2 to 3.0 times of rated voltage, or a range between 1.14:1 to 1.24:1. While the 2V rated PA capacitor made by manufacturer E, shows a range ratio of 3.5 to 4.7. One of the most interesting results showing in Figure 11 is that all capacitors exhibit nearly identical value of slope β (from 27.01 to 32.19) in the Weibull statistical plot for surge breakdown voltage, clearly indicating an identical failure mechanism in all PA capacitors.

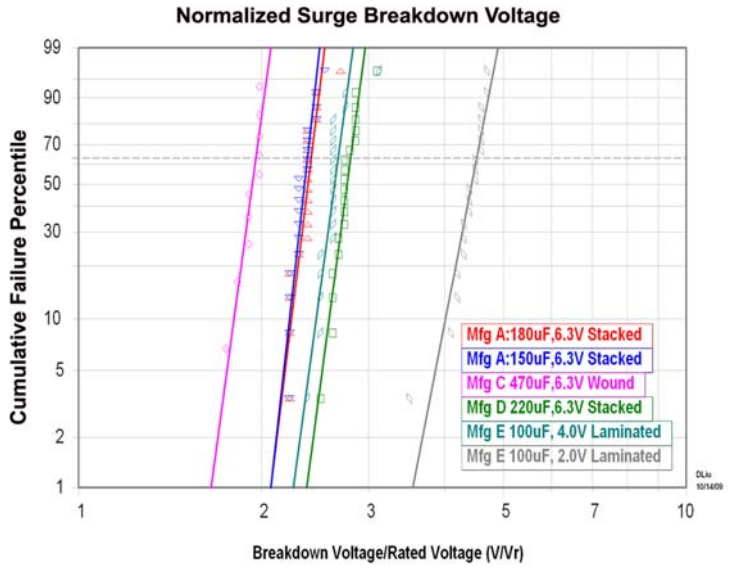

Figure 11. Normalized SSST breakdown voltages for 6.3V and lower rated voltage PA capacitors made by different manufacturers and with different physical structures. The surge breakdown voltage shows nearly identical value of slope β (from 27.01 to 32.19).

The surge breakdown voltages of 4V and 2V PA capacitors with a "laminated" structure are shown in Figure 12. The breakdown voltage data of a 4V, solid MnO_2-based tantalum capacitor is also used for comparison purpose. The Weibull r^2 probability distribution functions (PDF) plots of three capacitors are also shown in the right in Figure 12. This plot clearly shows the tight distributions in surge breakdown voltage in PA capacitors.

On the other hand, the average surge breakdown voltage of 4V solid MnO_2-based tantalum capacitor is higher than that of the same 4V rated PA capacitor, but with a much looser distribution, which indicates a higher probability of early failures in applications subject to current surges. On the other hand, the tight distribution of surge breakdown voltage in PA capacitors suggests that voltage de-rating may not be necessary for PA capacitors. Further investigation of the subject is in progress.

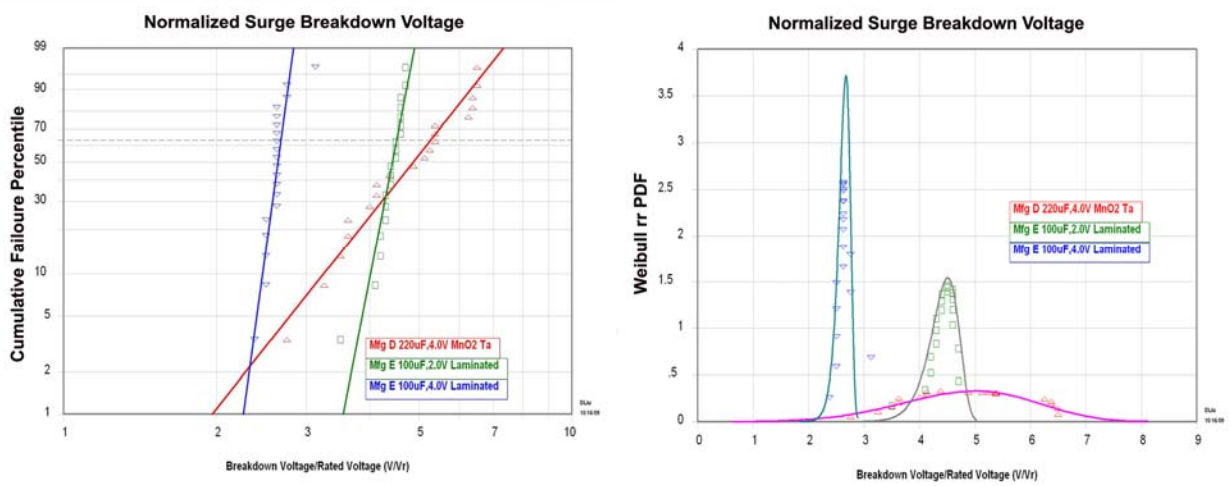

Figure 12. Normalized SSST breakdown voltages for 4V and 2V, 100 μF PA capacitors made by manufacturer E and for 4V, 220 μF, MnO_2-based tantalum capacitor made by manufacturer D. The Weibull probability distribution function plot (right) clearly shows the tight distribution in surge breakdown voltages in PA capacitors.

SUMMARY

Preliminary structure-property relationships in polymer aluminum (PA) capacitors are presented in this study. The physical structure of PA capacitors varies with manufacturers. Three different PA capacitor structures are revealed: traditional wound, stacked, and laminated.

Although all PA capacitors exhibit high capacitance and mΩ level low ESR values regardless of the capacitor structures, other electrical performance of PA capacitors depends highly on the capacitor structures. The PA capacitors made with loose wound structure show high dielectric loss, high DC leakage current, low capacitance roll-off frequency, and low surge breakdown voltages. The capacitors with "laminated" structure exhibit the most stable dielectric response versus frequency and temperature.

All PA capacitors show the same failure mechanism in surge breakdown voltage testing regardless of the capacitor structures. The much tighter distribution in surge breakdown voltages of PA capacitors, when compared to that of a MnO_2-based tantalum capacitor, suggests that voltage de-rating may not be necessary for PA capacitors.

REFERENCE

[1] Erik Reed, Characterization of Tantalum Polymer Capacitors, NASA NEPP reports (2005, 2006)
[2] Erik Reed, J. Kelly, L. Paulson, Reliability of Low-Voltage Tantalum Polymer Capacitors, CARTS USA 2005, 189-198.
[3] A. Nishino, J. of Power Sources 60 (1996) 137-147.
[4] Y. Kudoh, T. Kojima, S. Tsuchiya, S. Yoshimura, J. Power Sources 60 (1996) 157-163
[5] J. Prymak, Improvements with Polymer Cathodes in Aluminum and Tantalum Capacitors. IEEE Applied Power and Electronic Conference, Anaheim, CA (2001) p1210-18
[6] J. Martins, S. Costa, M. Bazzaoui, J. of Power Sources 160 (2006) 1471-79.
[7] J. Marshall and J. Prymak, Surge Step Stress Testing (SSST) of Tantalum Capacitors, CARTS 2001, 181-187.